Ru K-edge absorption study on the $La_{1-x}Ce_xRu_2$ system

2000 J. Phys.: Condens. Matter 12 6971

(http://iopscience.iop.org/0953-8984/12/30/324)

J. Phys.: Condens. Matter **12** (2000) 6971–6978. Printed in the UK PII: S0953-8984(00)12674-8

Ru K-edge absorption study on the $La_{1-x}Ce_xRu_2$ system

Ziyu Wu†, N L Saini†, S Agrestini†, D Di Castro†, A Bianconi†, A Marcelli‡, M Battisti‡, D Gozzi§ and G Balducci§

† Dipartimento di Fisica, Università di Roma 'La Sapienza', and Unità INFM, Piazzale Aldo Moro 2, 00185 Roma, Italy
‡ Laboratori Nazionali di Frascati, INFN, 00044, Frascati, Italy
§ Dipartimento di Chimica, Università di Roma 'La Sapienza', Piazzale Aldo Moro 2, 00185 Roma, Italy

Received 17 March 2000, in final form 25 May 2000

Abstract. We have measured high-resolution Ru K-edge x-ray absorption spectra for the intermetallic $La_{1-x}Ce_xRu_2$ system. Multiple-scattering calculations are made to explore the origins of different features observed in the experimental x-ray absorption near-edge structure (XANES) and their variation with Ce doping. The experiments and theoretical analysis demonstrate that the Ce doping in $La_{1-x}Ce_xRu_2$ has a direct influence on the states at the Fermi level and hence the hybridization between the f and d states induced by doping.

1. Introduction

The hybridization of localized f electrons (magnetism) and itinerant d electrons (superconductivity) drives intermetallics towards the borderline between magnetic and metallic systems. A particular type of superconducting phase appears, with coexistence of magnetism and superconductivity. Among the Ce-based intermetallics, $CeRu_2$ has attracted significant attention due to its anomalous electronic ground state [1–4]. A conventional argument that the superconductivity in $CeRu_2$ ($T_c = 6.2$ K) is solely derived from the Ru 4d electrons has been refuted by several spectroscopic experiments revealing mixed-valence Ce with significant weight of f states at the Fermi level [2–5]. Indeed $CeRu_2$ represents an interesting example among the intermetallic superconductors, where the f electrons present both localized and itinerant character, forming an appreciably wide 4f band [3, 4]. In fact, unlike the uranium-based heavy-fermion compounds, $CeRu_2$ is a magnetic superconductor with an extremely small magnetic moment due to the strong hybridization and hence the itinerant character of the f electrons. There have been some efforts made towards achieving an understanding of the nature of itinerant and localized f electrons, by studying substitution effects that in turn could give clues about the unconventional superconductivity in the $CeRu_2$ system. In fact, magnetic and non-magnetic substitutions for Ce in $CeRu_2$ are found to influence the characteristic properties of the system differently [5–9].

$LaRu_2$ provides an interesting case [6, 9–11] since it is formally a $4f^0$ system showing a superconducting transition at 4.4 K. Systematic studies of Ce substitution in $La_{1-x}Ce_xRu_2$ have shown an anomalous evolution of the superconducting transition temperature from $T_c \sim 4.4$ K at $x = 0.0$ to $T_c \sim 0.3$ K at $x \sim 0.5$. The lattice parameters are found to show a continuous evolution with substitution of Ce, indicating an average compression of the unit cell [6]. The cooling of the sample introduces a further compression of the unit cell, showing overall flexibility of the lattice structure. The anomalous lattice flexibility of $CeRu_2$ was further

0953-8984/00/306971+08$30.00

shown by an ultrasonic technique measuring the elastic stiffness, that shows significant lattice softening without structural transition in the normal state [12]. It is unusual, however, in that similar kinds of lattice anomalies are found in the high-T_c superconductors showing anomalous lattice flexibility as a function of temperature without any average structural transformation [13, 14]. Furthermore, the importance of the lattice in the electronic properties has been indicated by an abnormal pressure dependence of the superconducting transition temperature of the $La_{1-x}Ce_xRu_2$ system. T_c decreases linearly with increasing pressure in the small-pressure region <0.5 GPa; however, there is an increase in T_c while the pressure is in the region of 1 GPa. Obviously this unusual effect of pressure on T_c indicates an interesting evolution of the electron–lattice interactions in the $La_{1-x}Ce_xRu_2$ superconductor [8].

It still remains to be understood whether the decrease of T_c in $La_{1-x}Ce_xRu_2$ is due to increasing magnetic interaction or due to change in the local electronic density of states and/or local lattice distortions. X-ray absorption spectroscopy is a probe of both local electronic density and the local lattice [15], and could be exploited to explore these effects in the Ce intermetallics. The x-ray absorption coefficient $\mu(E)$ is given by the product of the matrix element and the joint density of states for the electronic transitions from the initial to final states. It can be solved in the real space for electronic transitions from an initial localized core level to a final state described as an outgoing spherical wave which interferes with the waves back-scattered from the neighbouring atoms [15]. The timescale of the x-ray absorption technique, which is related to the lifetime of the excited photoelectron, is of the order of 10^{-15} s, making the technique a very fast probe compared to others, allowing one to study instantaneous local lattice fluctuations, in addition to the local electronic structure. Here we report high-resolution Ru K-edge x-ray absorption near-edge structure (XANES) studies on the $La_{1-x}Ce_xRu_2$ system, to provide further progress towards understanding the role of local electronic and lattice structure. A real-space analysis of the XANES spectra has been made. It is shown that the Ce doping in $La_{1-x}Ce_xRu_2$ has a direct influence on the states at the Fermi level and hence the hybridization between the f and d states due to local lattice distortions induced by doping.

2. Experimental procedure

Ru K-edge absorption measurements were performed on well characterized powder samples of $La_{1-x}Ce_xRu_2$ prepared using arc melting under argon atmosphere, followed by high-temperature vacuum homogenization. The details of the samples and their characterization can be found elsewhere [5]. The fluorescence-yield (FY) high-resolution absorption measurements were made at the beamline BM29 of the European Synchrotron Radiation Facility (ESRF), Grenoble, using a Si(311) double-crystal monochromator. The Ru Kα fluorescence yield was collected using a multi-element Ge x-ray detector array covering a large solid angle of the x-ray fluorescence emission. The temperature-dependent measurements were performed on the samples mounted in a closed-cycle He refrigerator. The sample temperature was controlled by a PID controller and monitored with an accuracy of ± 1 K. Several absorption scans at the same temperature were recorded to ascertain the reproducibility and to obtain spectra with very high signal-to-noise ratio.

3. Calculation details

The multiple-scattering (MS) calculations, based on one-electron full MS theory, were carried out [16–19] using the CONTINUUM code [20]. We have used the Mattheiss prescription [21]

to construct the cluster electronic density and the Coulomb part of the potential by superposition of neutral atomic charge densities obtained either from the Clementi–Roetti tables for Ru atoms [22] or generated by the atomic relativistic Hartree–Fock–Slater code of Desclaux for La and Ce [23]. In order to simulate the charge relaxation around the core hole in the photoabsorber of atomic number Z, we have used the screened $Z+1$ approximation (final-state rule) [24], which consists in taking the orbitals of the $Z+1$ atom and in constructing the final-state charge density by using the excited configuration of the photoabsorber with the core electron promoted to a valence orbital.

For the exchange–correlation part of the potential, we have used the energy- and position-dependent complex Hedin–Lundquist (H–L) self-energy $\Sigma(r, E)$ as illustrated by Tyson *et al* [25]. The imaginary part of the H–L potential gives the amplitude attenuation of the excited photoelectron wave due to extrinsic inelastic losses, and automatically takes into account the photoelectron mean free path in the excited final state. The calculated spectra are further convoluted with a Lorentzian function with a full width $\Gamma_h = 5.5$ eV to account for the Ru 1s core-hole lifetime and a Gaussian function due to experimental resolution. Similar results are obtained by performing the calculation using an X_α-type of exchange-energy-dependent Lorentzian convolution to account for inelastic losses of the photoelectron in the final state and the core-hole lifetime. In the latter, the total width of the Lorentzian is given by $\Gamma_{tot}(E) = 2I_m\Sigma(E)$ where $\Sigma(E)$ is a volume-averaged value for the unit cell, $\Sigma(r, E)$, convoluted with the experimental Gaussian width. We have chosen the muffin-tin radii according to the criterion of Norman [26], allowing a 10% overlap between contiguous spheres to simulate the atomic bond.

4. Results and discussion

Figure 1 shows a high-resolution Ru K-edge XANES spectrum measured at 200 K for $LaRu_2$ by collecting the fluorescence photons emitted from the sample. The atomic absorption jump at the edge is normalized to one. The well resolved peaks in the XANES spectrum are denoted

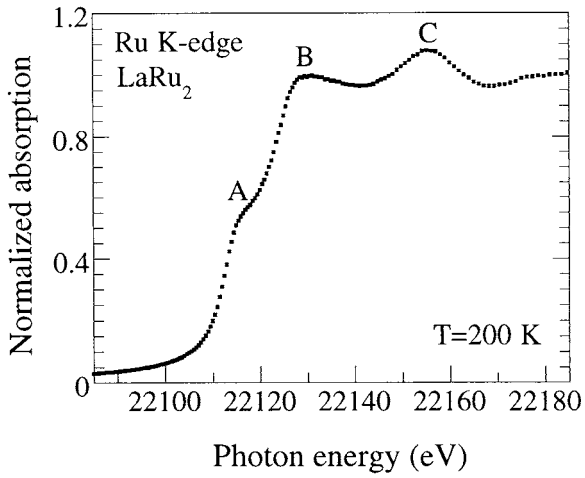

Figure 1. The Ru K-edge x-ray absorption near-edge structure (XANES) spectrum measured at 200 K for $LaRu_2$ in the fluorescence-yield mode. The spectrum is normalized to the atomic absorption.

by A, B and C. The peak positions were precisely determined from the second derivative of the spectrum. The peak A appears near the threshold of the Ru K edge. The peak B appears at about 12 eV above the threshold while the peak C appears at about 38 eV above the threshold.

$La_{1-x}Ce_xRu_2$ has a Laves phase structure which is a face-centred cubic ($MgCu_2$-type) structure [1]. We have calculated the real-space multiple scattering of the photoelectron excited from the Ru 1s state to the atoms surrounding the central Ru for a cluster of atoms. Figure 2 shows the Ru K-edge XANES spectra for $LaRu_2$ calculated using full multiple scattering with a relaxed final-state potential for different clusters of increasing size up to the convergence (two, three, four and five shells). The five-shell spectrum contains all atoms within 5 Å from the central Ru.

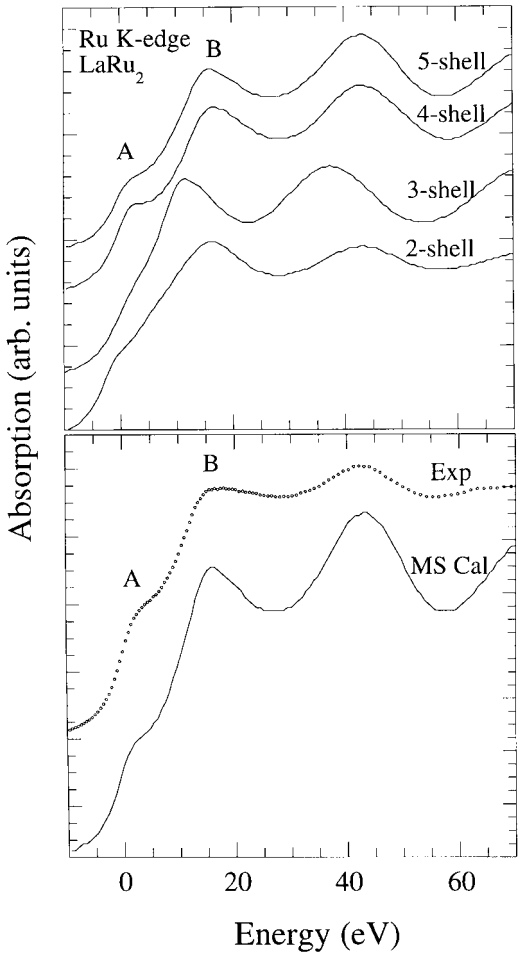

Figure 2. Multiple-scattering calculations of Ru K-edge XANES spectra for $LaRu_2$ as functions of the cluster size (upper). The calculated XANES spectrum for the five-shell cluster is compared with the experimental spectrum. The zero of the energy scale in the experimental spectrum is fixed to the Ru 1s threshold.

The calculated absorption spectrum for the minimum size of the cluster, containing the central Ru atom surrounded by the six neighbouring Ru atoms sited at about 2.72 Å, shows two broad peaks B and C, and a weak peak A. As the spectrum should reflect the local empty density of states of p symmetry, the feature B can be assigned to the $1s \rightarrow 5p$ transition. In the real space, the feature B is attributable to multiple scattering within the Ru atomic shell while the peak C is dominantly due to single-scattering events involving the absorber and the shell of six Ru atoms.

The peak A is due to hybridization between the 5p states of the central Ru atom with the 4d orbitals of the surrounding Ru atoms in the second shell [27]. When the third shell containing La is added, the spectrum does not show a large change except the smearing in the pre-edge region, because the electron cloud around the La shares the hybridization due to the binding between the third-shell La and the second-shell Ru atoms. When the cluster size is further increased by adding Ru atoms around the La, the ligand field around the photoabsorber Ru is formed and hence an increase of peak A occurs.

The experimental features are well reproduced in the calculated spectrum with a cluster including five shells. Indeed the agreement of the calculated and experimental spectra is impressive as regards the intensity and the energy positions (figure 2). Thus it is reasonable to assume that the cluster including four to five shells is sufficient to describe the main characteristics of the Ru K-edge XANES and hence the properties of the system under study.

It is worth recalling that XANES spectra are influenced by final-state core-hole potential effects. Here we have investigated the validity of the different approaches for the case of the Ru K edge with respect to core-hole potential effects. For this purpose we have performed the MS calculations considering the case of a fully relaxed final-state potential, the $Z + 1$ approximation accounting for the core-hole potential in the final state, and the case in which the final-state potential remains unrelaxed. The outcomes of the two approaches for the case of $LaRu_2$ are shown in figure 3. There are significant differences between the two calculations, suggesting the final-state core-hole potential effects to be important for the Ru K edge. The calculation based on the $Z + 1$ approximation shows better agreement with the experimental results, and hence the relaxed potential approximation used for the calculations reported in this work is justified.

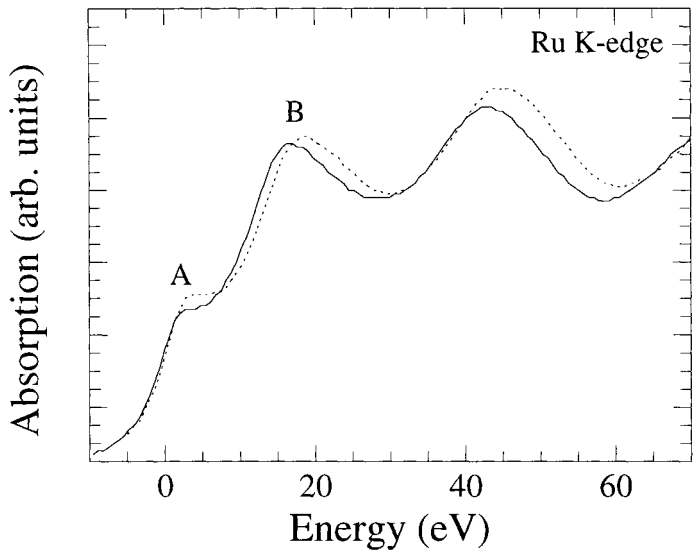

Figure 3. Multiple-scattering calculations of the Ru K-edge XANES spectra for $LaRu_2$ taking a fully relaxed final-state potential using the $Z + 1$ approximation (solid line) compared with the case for the unrelaxed potential (dotted line).

In order to explore the origin of the peak A for $LaRu_2$ we have made further calculations. Figure 4 shows a comparison of the calculated spectrum obtained considering a simplified cluster of 19 atoms with an artificially suppressed first-nearest-Ru shell and the spectrum

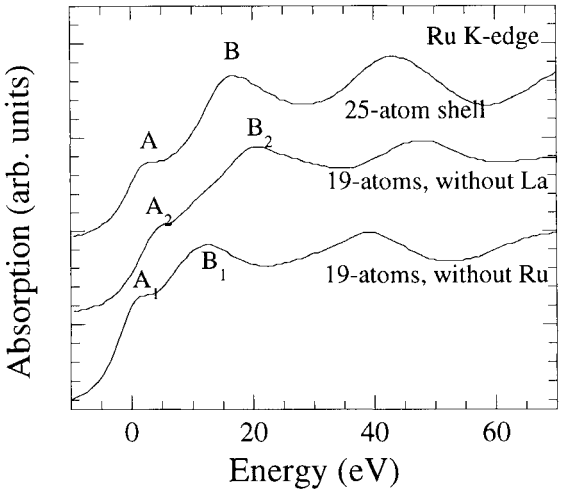

Figure 4. Multiple-scattering calculations of Ru K-edge XANES for $LaRu_2$ using simplified atomic clusters: (a) the calculated spectrum for a cluster of four shells (see, e.g., figure 3) with a suppressed first Ru shell and (b) that with a suppressed second La shell; (c) the four-shell cluster results are shown (as in figure 3) for easy reference.

calculated with a suppressed La shell. The calculated spectrum for a cluster of four shells, showing good agreement with the experimental spectrum, is also shown for easy reference. The spectrum with the suppressed Ru shell shows a clear peak (denoted here by A_1)—however at a slightly energy-shifted position—but the main absorption feature (denoted here by B_1) shows a large change in its energy position. On the other hand, the spectrum with the suppressed La shell shows a spectrum with the main peak shifted toward high energy by $\sim$3 eV and a broadened pre-edge peak shifted slightly towards the higher-energy side. This result clarifies the origin of the pre-peak, suggesting that the peak A should be associated with the unoccupied states made up of mixed Ru p–d states, i.e. central Ru 5p states hybridized with d orbitals of the outer Ru shell. These states also appear to be mixed with higher-shell La d/f electronic orbitals. Figure 4 further suggests that the neighbouring atoms strongly interact with each other, causing the molecular orbitals to overlap forming extended energy bands and modifying their position near the Fermi level.

Now we turn to the influence of Ce doping on the local electronic density of states and the local lattice displacements in the $La_{1-x}Ce_xRu_2$ system. Figure 5 shows the absorption difference between the spectra measured for $La_{0.5}Ce_{0.5}Ru_2$ and $LaRu_2$ at 200 K (symbols). We observe a sharp decrease of the unoccupied density of states at the Fermi level (α) and a complex variation of the spectral features in energy range up to $\sim$50 eV. In order to understand the spectral variations, we have calculated the XANES spectra taking into account just the compression of the crystalline lattice (from 7.7 Å to 7.63 Å as given in [6]). We have shown the difference between the spectra for the compressed and uncompressed $LaRu_2$ lattice in figure 5 (solid line). The effect of the compression on the XANES is well reproduced in the energy range 10–50 eV. On the other hand, the experimental variation in the density of states at the Fermi level could not be reproduced in the calculations. We have made a further effort to simulate the effect of substitution of Ce for La in the native $LaRu_2$, considering the nominal composition $La_{0.5}Ce_{0.5}Ru_2$ where the compression (Ce is smaller than La) and the electronic configuration of Ce are taken into account.

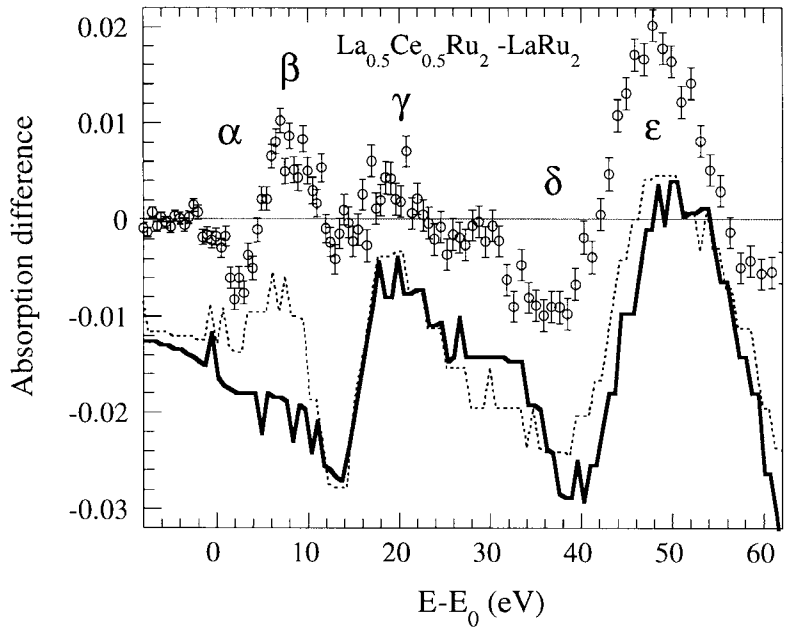

Figure 5. The absorption difference between the normalized spectra of $LaRu_2$ and $La_{0.5}Ce_{0.5}Ru_2$ at 200 K (symbols): the difference between the calculated spectra for $LaRu_2$ and $La_{0.5}Ce_{0.5}Ru_2$ (dotted line) and the difference between the calculated spectra for $LaRu_2$ and the compressed lattice of $LaRu_2$ (solid line).

The absorption difference between the spectra calculated for $La_{0.5}Ce_{0.5}Ru_2$ and $LaRu_2$ is plotted (dotted line). The agreement of experiment and calculations is improved and we can reproduce the variation of the peak β; however, we do not observe the sharp drop in the α-peak at the Fermi level. This suggests that the substitution of Ce in place of La does not change the one-electron density of states at the Fermi level, as shown by the multiple-scattering calculations. Therefore the disagreement between the calculated and experimental differences is presumed to be related to a renormalization of quasi-particles.

In summary, we have made high-resolution Ru K-edge XANES measurements on the $La_{1-x}Ce_xRu_2$ system to investigate the influence of Ce doping on the local electron density of states. A real-space multiple-scattering approach has been used to identify the XANES features. A direct comparison of experimental and calculated spectra has been made to explore the origins of different experimental features, allowing us to study the changes due to the Ce doping in the native $LaRu_2$ lattice. The *ab initio* theoretical simulation, made in terms of various simplified cluster models, provides a direct description of the origins of various features observed in the experimental spectrum. The results suggest that structural displacements around the Ru site play an important role in determining the local electronic structure near the Fermi level of the $LaRu_2$ compound. Good agreement between the experiment and the single-particle theoretical description at a few eV above the Fermi level has been found both for the native system and for the Ce-substituted material. We have found experimentally a suppression of the spectral weight at the Fermi level in $La_{0.5}Ce_{0.5}Ru_2$ that could explain the decrease of the superconducting transition temperature. It appears not to be related to the variation of the single-particle density of states, but it could be due to a renormalization of quasi-particles at the Fermi level.

Acknowledgments

This research was supported by the Ministero dell'Università e della Ricerca Scientifica (MURST) under the Programmi di Ricerca Scientifica di Rilevante Interesse Nazionale coordinated by R Ferro, by Istituto Nazionale di Fisica della Materia (INFM) and by Progetto 5% Superconduttività del Consiglio Nazionale delle Ricerche (CNR).

References

[1] Huxley A D, Dalmas de Réotier P, Yaouanc A, Caplan D, Couach M, Lejay P, Gubbens P C M and Mulders A M 1996 *Phys. Rev.* B **54** R9666
Huxley A D, Boucherle J X, Bonnet M, Bourdarot F, Schustler I, Caplan D, Lelievre E, Bernhoeft N, Lejay P and Gillon B 1997 *J. Phys.: Condens. Matter* **9** 4185
[2] Allen J W, Oh S J, Lindau I, Maple M B, Suassuna J F and Hagström S B 1982 *Phys. Rev.* B **26** 445
[3] Yang S-H, Kumigashira H, Yokoya T, Chainani A, Takahashi T, Takeya H and Kadowaki K 1996 *Phys. Rev.* B **53** R11 946
[4] Kang J S, Olson C G, Edo M, Inada Y, Onuki Y, Kwon S K and Min B I 1999 *Phys. Rev.* B **60** 5348
[5] Battisti M, Marcelli A, Chudinov S, Bozukov L, Piquer C and Chaboy J 2000 *J. Magn. Magn. Mater.* at press
Battisti-Laurea M 2000 *Thesis* Università di Roma 'La Sapienza'
[6] Shelton R N, Lawson A C and Baberschke K 1977 *Solid State Commun.* **24** 465
[7] Roy S B 1992 *Phil. Mag.* **65** 1435
Roy S B, Pradhan A K and Chaddah P 1996 *Physica* C **271** 181
[8] Nakama T, Hedo M, Maekawa T, Higa M, Resel R, Sugawara H, Settai R, Onuki Y and Yagasaki K 1995 *J. Phys. Soc. Japan* **64** 1471
Nakama T, Uwatoko Y, Kohama T, Bukov A T, Mori N, Yoshida H, Abe S, Kaneko T and Yagasaki K 1998 *Rev. High Pressure Sci. Technol.* **7** 632
[9] Chudinov S, Brando M, Marcelli A and Battisti M 1998 *Physica* B **244** 154
[10] Rettori C, Davidov D, Chaikin P and Orbach R 1973 *Phys. Rev. Lett.* **30** 437
[11] Asokamani R, Subramanian G, Mathi Jaya S and Pauline S 1991 *Phys. Rev.* B **44** 2283
[12] Suzuki T, Goshima H, Sakita S, Fujita T, Hedo M, Inada Y, Yamamoto E, Haga Y and Onuki Y 1996 *J. Phys. Soc. Japan* **65** 2753
[13] Nohara M, Suzuki T, Maeno Y, Fujita T, Tanaka I and Kojima H 1993 *Phys. Rev. Lett.* **70** 3447
Nohara M, Suzuki T, Maeno Y, Fujita T, Tanaka I and Kojima H 1995 *Phys. Rev.* B **52** 570
[14] Bianconi A, Saini N L, Lanzara A, Missori M, Rossetti T, Oyanagi H, Yamaguchi H, Oka K and Ito T 1996 *Phys. Rev. Lett.* **76** 3412
[15] Bianconi A 1988 *X-ray Absorption: Principles, Applications, Techniques of EXAFS, SEXAFS, XANES* ed R Prinz and D Koningsberger (New York: Wiley)
[16] Durham P J 1988 *X-ray Absorption: Principles, Applications, Techniques of EXAFS, SEXAFS, XANES* ed R Prinz and D Koningsberger (New York: Wiley)
[17] Bianconi A and Marcelli A 1992 *Synchrotron Radiation Research: Advances in Surface Science* ed R Z Bachrach (New York: Plenum)
[18] Bianconi A, Garcia J and Benfatto M 1988 *Springer Topics in Current Chemistry 145* ed E Mandelkow (Berlin: Springer) p 29
Bianconi A, Garcia J, Marcelli A, Benfatto M, Natoli C R and Davoli I 1985 *J. Physique Coll.* **46** C9 101
Benfatto M, Natoli C R, Bianconi A, Garcia J, Marcelli A, Fanfoni M and Davoli I 1986 *Phys. Rev.* B **34** 5774
[19] Wu Z Y, Benfatto M and Natoli C R 1992 *Phys. Rev.* B **45** 531
Wu Z Y, Benfatto M and Natoli C R 1993 *Solid State Commun.* **87** 475
[20] Natoli C R, unpublished
[21] Mattheiss L 1964 *Phys. Rev.* A **134** 970
[22] Clementi E and Roetti C 1974 *At. Data Nucl. Data Tables* **14**
[23] Desclaux J 1975 *Comput. Phys. Commun.* **9** 31
Desclaux J 1971 *J. Phys. B: At. Mol. Phys.* **4** 631
[24] Lee P A and Beni G 1977 *Phys. Rev.* B **15** 2862
[25] Tyson T A, Hodgson K O, Natoli C R and Benfatto M 1992 *Phys. Rev.* B **46** 5997
[26] Norman J G 1974 *Mol. Phys.* **81** 1191
[27] Wu Z Y, Jollet F and Gautier-Soyer M 1999 *J. Phys.: Condens. Matter* **11** 7185